## Supplementary Materials

## Figure S1

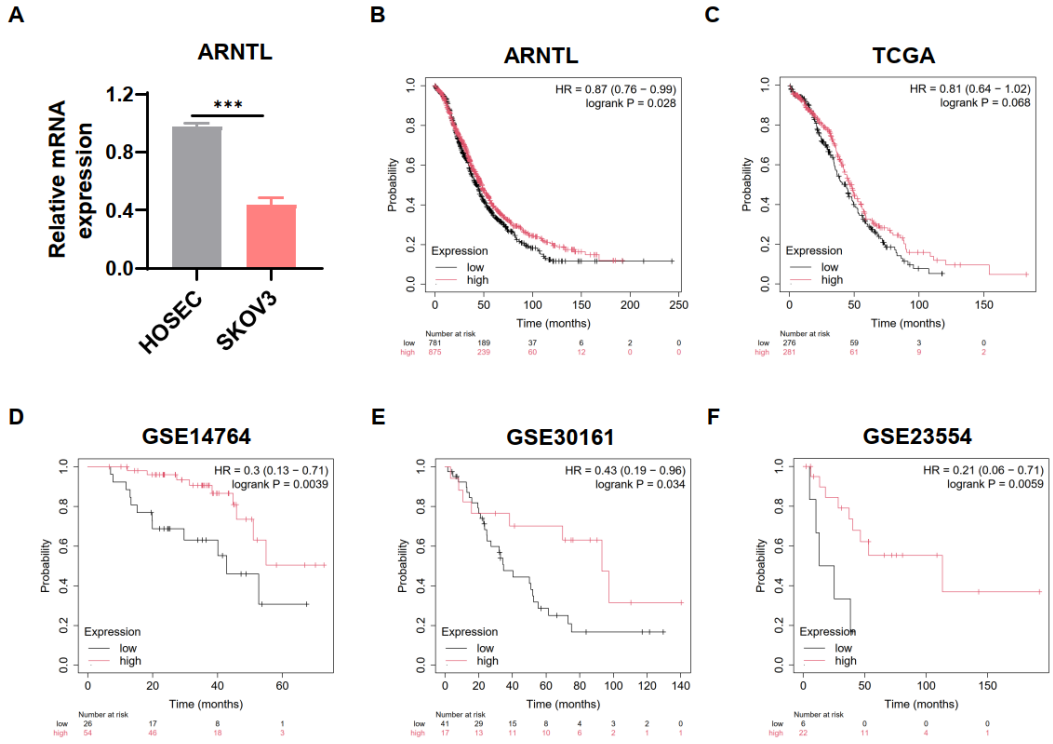


**Figure S1:** The Real-time qPCR analysis was adopted to evaluate the expression of ARNTL in SKOV3 compared with HOSEC as normal control(A). Kaplan-Meier analysis for overall survival in ARNTL expressed in ovarian cancer patients, covering Kaplan-Meier Plotter (B), and TCGA (C), GSE147641 (D), GSE30161 (E), GSE23554 (F). Logrank p-value<0.05 was considered statistically significant.

**Figure S2**

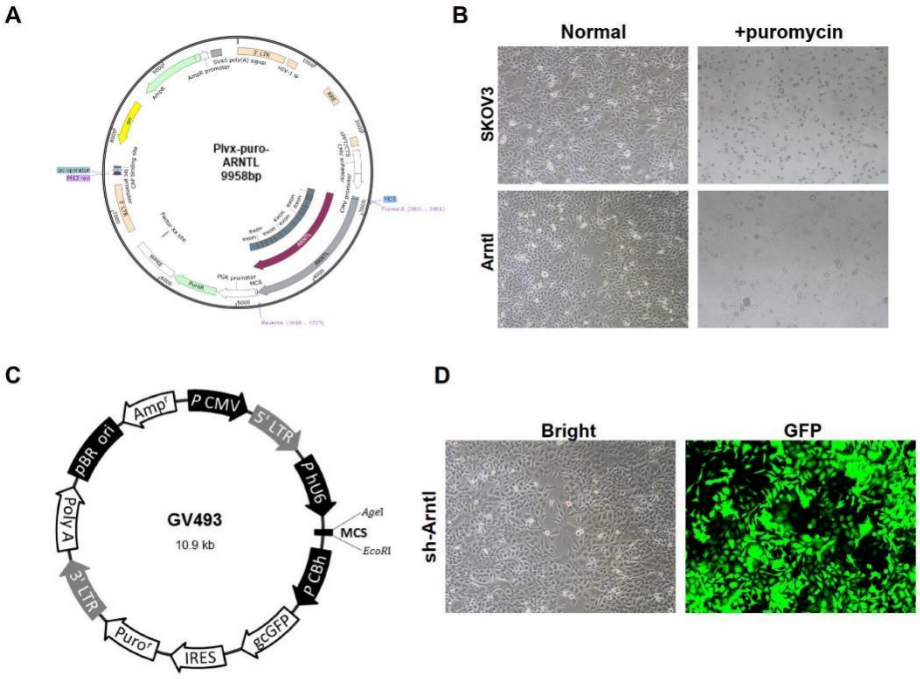


**Figure S2:** Cell construction. A, overexpression plasmid profile of ARNTL. B, Screening of puromycin. C, ARNTL's interference plasmid profile. D, Transfection efficiency of SKOV3 cell lentiviral vector.

**Figure S3**

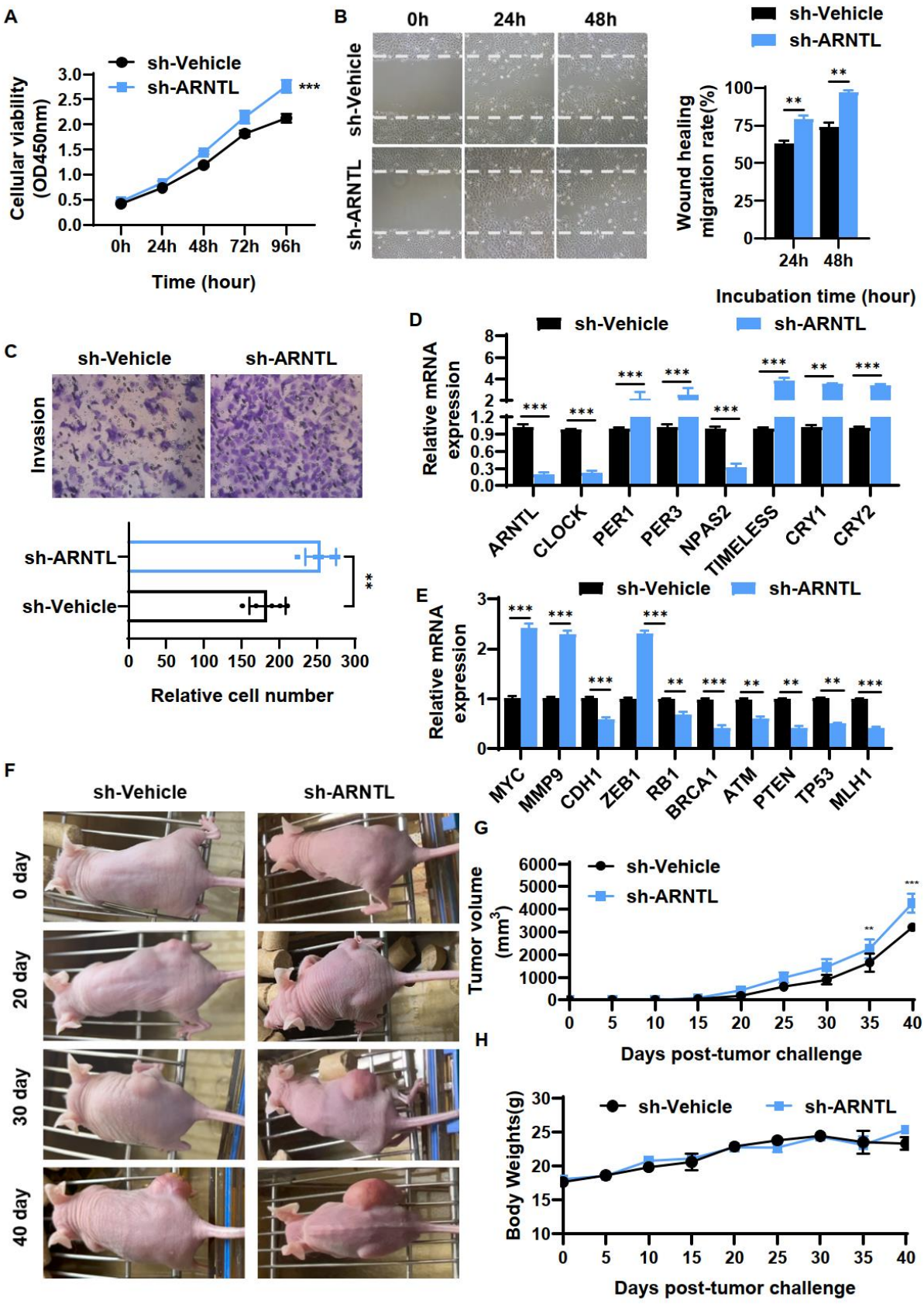
A
sh-Vehicle
sh-ARNTL
Cellular viability (OD450nm)
Time (hour)
0h 24h 48h 72h 96h
B
0h 24h 48h
sh-Vehicle
sh-ARNTL
Wound healing migration rate(%)
Incubation time (hour)
C
sh-Vehicle
sh-ARNTL
Invasion
Relative cell number
D
Relative mRNA expression
ARNTL CLOCK PER1 PER3 NPAS2 TIMELESS CRY1 CRY2
E
Relative mRNA expression
MYC MMP9 CDH1 ZEB1 RB1 BRCA1 ATM PTEN TP53 MLH1
F
0 day
20 day
30 day
40 day
G
Tumor volume (mm3)
Days post-tumor challenge
H
Body Weights(g)
Days post-tumor challenge

**Figure S3:** ARNTL inhibits ovarian cancer cell invasion and metastasis in vitro and in vivo. A, Relative growth rates of indicated cells determined by CCK8 assay. Values are mean ± SD (two-way ANOVA). B, Representative images for wound healing of indicated cells (left). Quantification of migration rate (right). Values are mean ± SD. C, Representative images for Transwell invasion assays of indicated cells (up), scale bar: 100 μm. Relative numbers of invasion cells (down). Values are mean ± SD. D, Real-time qPCR analysis for genes related to circadian rhythm in indicated cells. Values are mean ± SD. E, Real-time qPCR analysis for genes related to cell proliferation and migration in indicated cells. Values are mean ± SD. F-G, Representative images for dynamic detection of tumor volume growth in sh-ARNTL and sh-Vehicle cells after tumor formation. Values are mean ± SD. H, Body weight change curve of mice after sh-ARNTL and sh-Vehicle cells tumorigenesis.

**FigureS4**

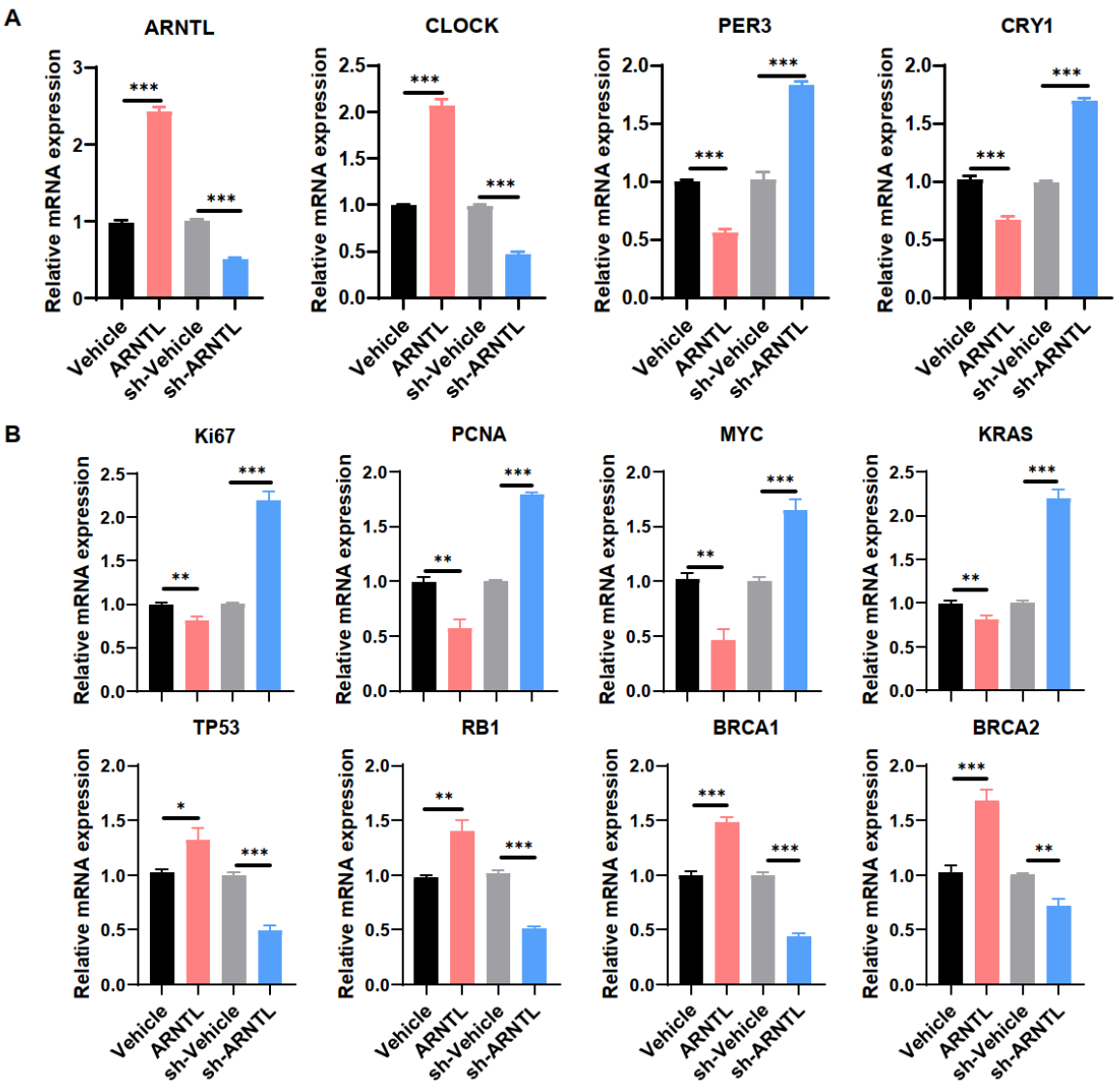


**FigureS4:** The expression of circadian rhythm and cell proliferation, invasion and metastasis genes. A, Real-time qPCR detection of circadian rhythm gene expression in indicated cells. B, Real-time qPCR detection of cell proliferation, invasion and metastasis genes expression in indicated cells.

# Figure S5

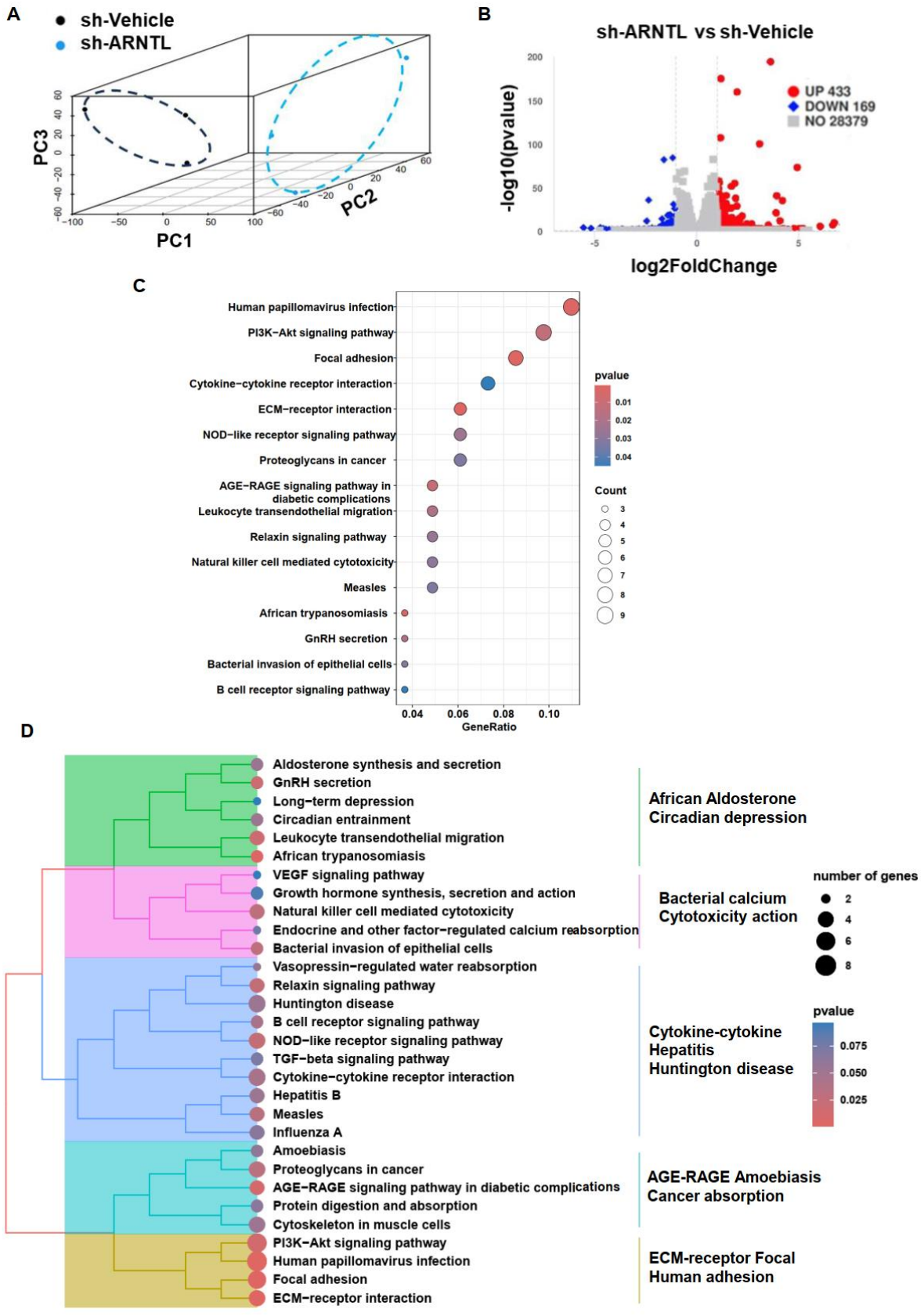
A
sh-Vehicle
sh-ARNTL
PC1
PC2
PC3
B
sh-ARNTL vs sh-Vehicle
UP 433
DOWN 169
NO 28379
-log10(pvalue)
log2FoldChange
C
Human papillomavirus infection
PI3K−Akt signaling pathway
Focal adhesion
Cytokine−cytokine receptor interaction
ECM−receptor interaction
NOD−like receptor signaling pathway
Proteoglycans in cancer
AGE−RAGE signaling pathway in diabetic complications
Leukocyte transendothelial migration
Relaxin signaling pathway
Natural killer cell mediated cytotoxicity
Measles
African trypanosomiasis
GnRH secretion
Bacterial invasion of epithelial cells
B cell receptor signaling pathway
GeneRatio
pvalue
Count
D
Aldosterone synthesis and secretion
GnRH secretion
Long−term depression
Circadian entrainment
Leukocyte transendothelial migration
African trypanosomiasis
VEGF signaling pathway
Growth hormone synthesis, secretion and action
Natural killer cell mediated cytotoxicity
Endocrine and other factor−regulated calcium reabsorption
Bacterial invasion of epithelial cells
Vasopressin−regulated water reabsorption
Relaxin signaling pathway
Huntington disease
B cell receptor signaling pathway
NOD−like receptor signaling pathway
TGF−beta signaling pathway
Cytokine−cytokine receptor interaction
Hepatitis B
Measles
Influenza A
Amoebiasis
Proteoglycans in cancer
AGE−RAGE signaling pathway in diabetic complications
Protein digestion and absorption
Cytoskeleton in muscle cells
PI3K−Akt signaling pathway
Human papillomavirus infection
Focal adhesion
ECM−receptor interaction
African Aldosterone
Circadian depression
Bacterial calcium
Cytotoxicity action
Cytokine-cytokine
Hepatitis
Huntington disease
AGE-RAGE Amoebiasis
Cancer absorption
ECM-receptor Focal
Human adhesion
number of genes
pvalue

**Figure S5:** ARNTL modulate ovarian cancer cells by fibroblast related signaling pathway. A, Whole transcriptomes were subjected to MDS on expressed genes to assess sample diversity and relatedness in sh-ARNTL(blue) and Sh-Vehicle(black). B, Volcano plots represent DEGs between two group comparisons (sh-ARNTL:sh-Vehicle). Red dots indicate upregulation in DEG ($Log_2$FoldChange≥1; P value≤0.05), and blue dots indicate down regulation ($Log_2$Foldchange≤-1; P value≤0.05). C, Bubble map for KEGG pathway analysis associated with Co-DEGs (ranked by P value). D, Treeplot for KEGG pathway analysis (ranked by P value).

**Figure S6**

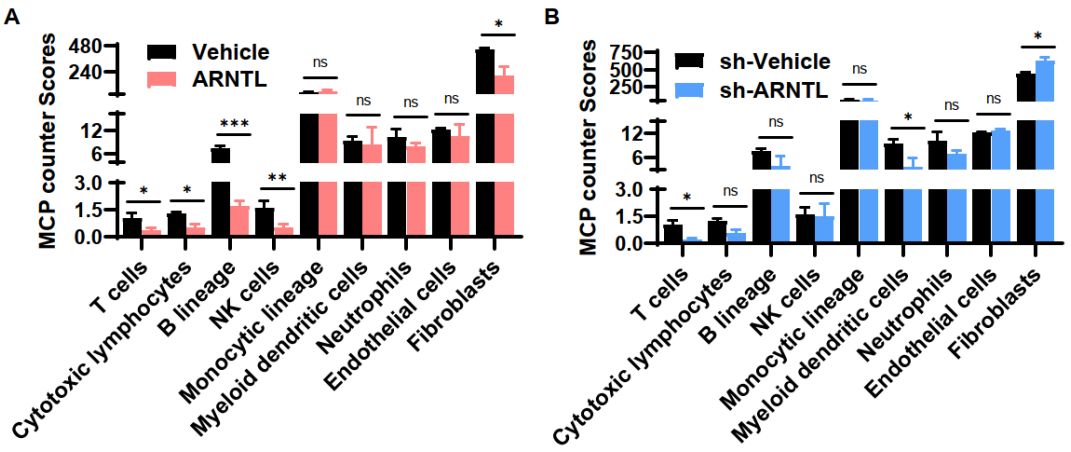


**Figure S6:** A-B, The MCP counter algorithm quantitatively deconvolves transcriptome data to estimate the absolute abundance of infiltrating immune and stromal populations in indicated group.

**Figure S7**

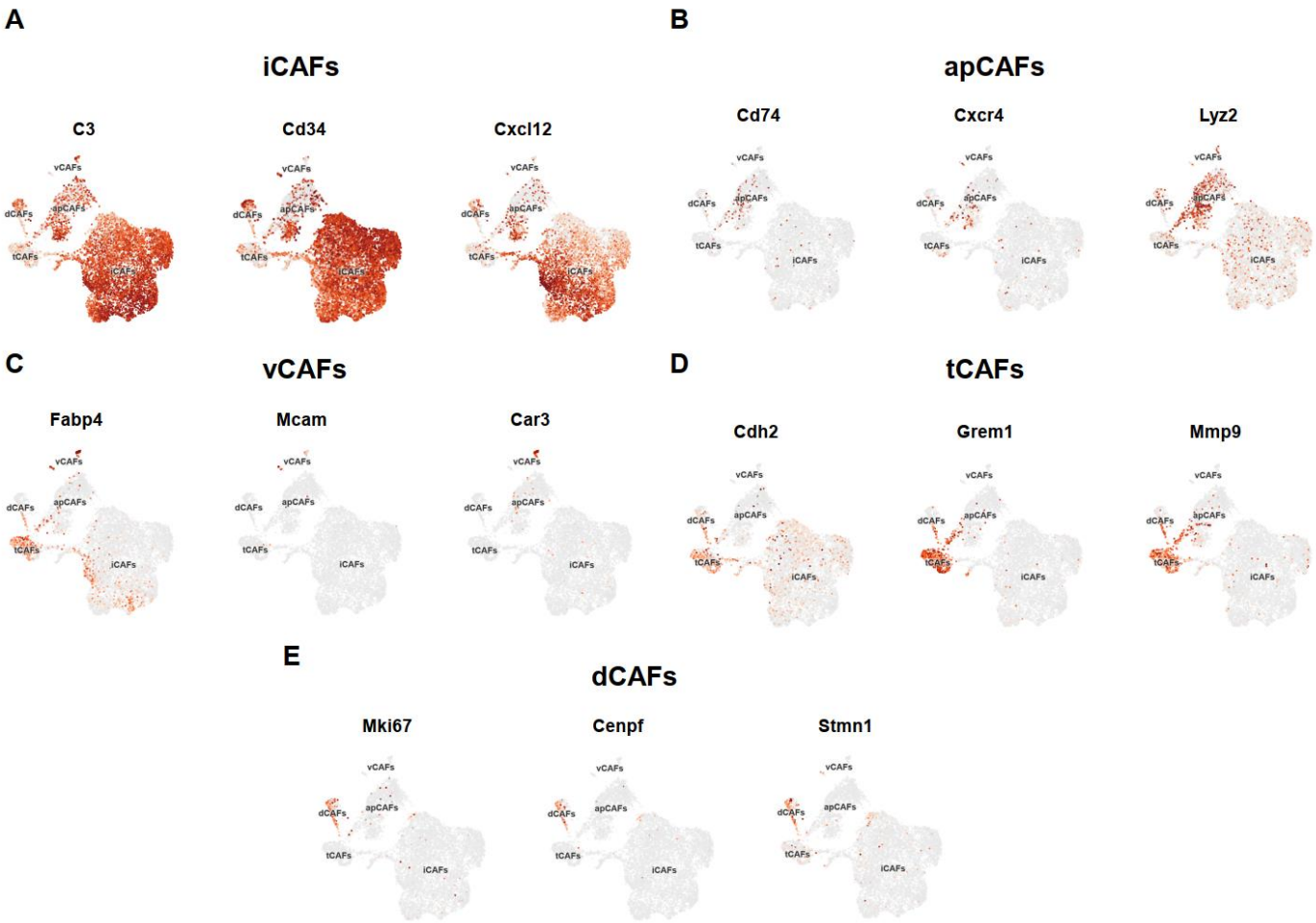


**Figure S7:** The expression distribution of typical marker genes for CAF subtypes in each CAF cluster. A, iCAFs; B, apCAFs; C, vCAFs; D, tCAFs; E, dCAFs.

# Figure S8

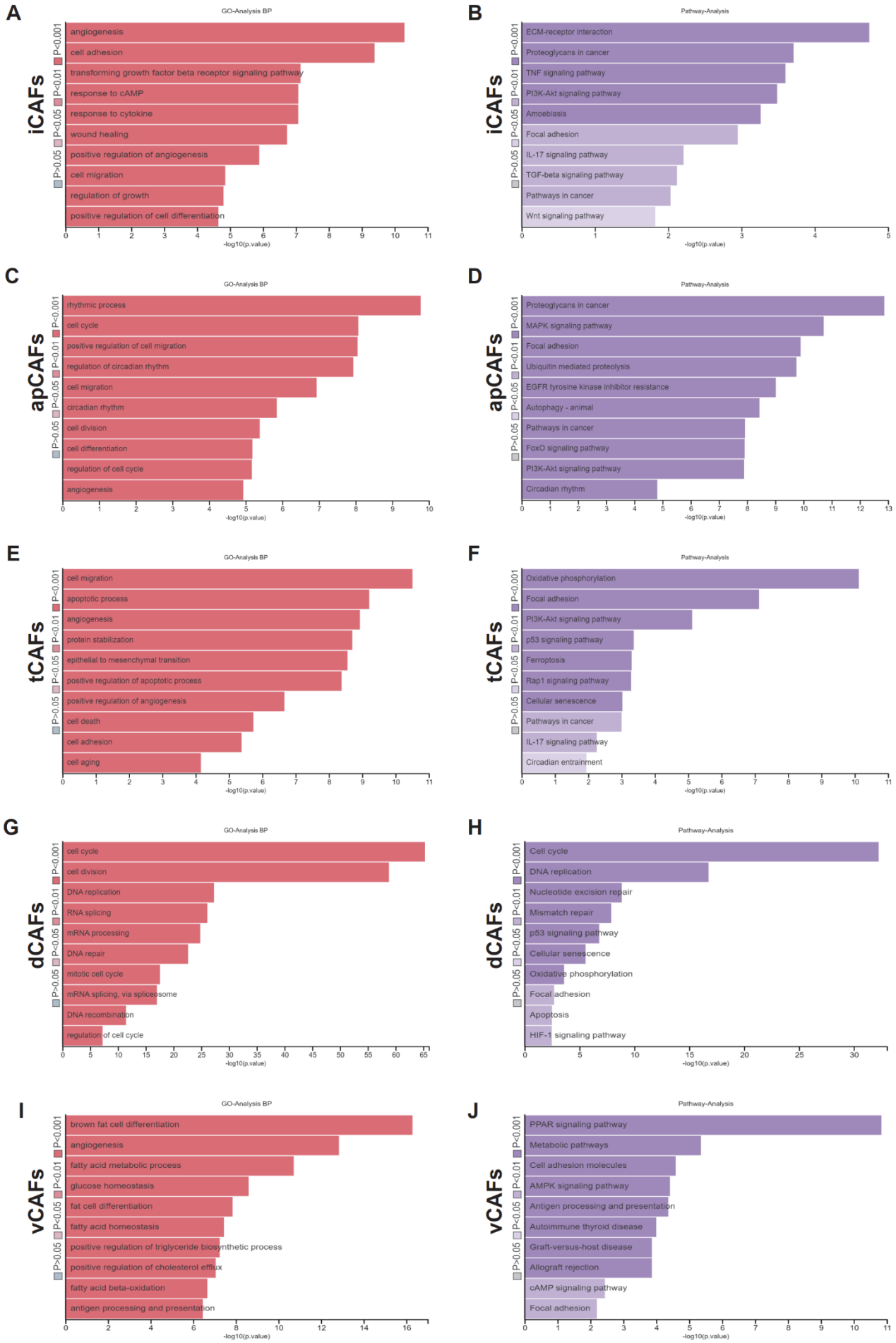
A
GO-Analysis BP
iCAFs
angiogenesis
cell adhesion
transforming growth factor beta receptor signaling pathway
response to cAMP
response to cytokine
wound healing
positive regulation of angiogenesis
cell migration
regulation of growth
positive regulation of cell differentiation
P<0.001
P<0.01
P<0.05
P>0.05
-log10(p.value)
B
Pathway-Analysis
iCAFs
ECM-receptor interaction
Proteoglycans in cancer
TNF signaling pathway
PI3K-Akt signaling pathway
Amoebiasis
Focal adhesion
IL-17 signaling pathway
TGF-beta signaling pathway
Pathways in cancer
Wnt signaling pathway
-log10(p.value)
C
GO-Analysis BP
apCAFs
rhythmic process
cell cycle
positive regulation of cell migration
regulation of circadian rhythm
cell migration
circadian rhythm
cell division
cell differentiation
regulation of cell cycle
angiogenesis
-log10(p.value)
D
Pathway-Analysis
apCAFs
Proteoglycans in cancer
MAPK signaling pathway
Focal adhesion
Ubiquitin mediated proteolysis
EGFR tyrosine kinase inhibitor resistance
Autophagy - animal
Pathways in cancer
FoxO signaling pathway
PI3K-Akt signaling pathway
Circadian rhythm
-log10(p.value)
E
GO-Analysis BP
tCAFs
cell migration
apoptotic process
angiogenesis
protein stabilization
epithelial to mesenchymal transition
positive regulation of apoptotic process
positive regulation of angiogenesis
cell death
cell adhesion
cell aging
-log10(p.value)
F
Pathway-Analysis
tCAFs
Oxidative phosphorylation
Focal adhesion
PI3K-Akt signaling pathway
p53 signaling pathway
Ferroptosis
Rap1 signaling pathway
Cellular senescence
Pathways in cancer
IL-17 signaling pathway
Circadian entrainment
-log10(p.value)
G
GO-Analysis BP
dCAFs
cell cycle
cell division
DNA replication
RNA splicing
mRNA processing
DNA repair
mitotic cell cycle
mRNA splicing, via spliceosome
DNA recombination
regulation of cell cycle
-log10(p.value)
H
Pathway-Analysis
dCAFs
Cell cycle
DNA replication
Nucleotide excision repair
Mismatch repair
p53 signaling pathway
Cellular senescence
Oxidative phosphorylation
Focal adhesion
Apoptosis
HIF-1 signaling pathway
-log10(p.value)
I
GO-Analysis BP
vCAFs
brown fat cell differentiation
angiogenesis
fatty acid metabolic process
glucose homeostasis
fat cell differentiation
fatty acid homeostasis
positive regulation of triglyceride biosynthetic process
positive regulation of cholesterol efflux
fatty acid beta-oxidation
antigen processing and presentation
-log10(p.value)
J
Pathway-Analysis
vCAFs
PPAR signaling pathway
Metabolic pathways
Cell adhesion molecules
AMPK signaling pathway
Antigen processing and presentation
Autoimmune thyroid disease
Graft-versus-host disease
Allograft rejection
cAMP signaling pathway
Focal adhesion
-log10(p.value)

**Figure S8:** Functional analysis in different CAFs. GO functional enrichment analysis of differentially expressed genes in iCAFs (A), apCAFs (C), tCAFs (E), dCAFs (G) and vCAFs (I). Pathway analysis of differentially expressed genes in iCAFs (B), apCAFs (D), tCAFs (F), dCAFs (H) and vCAFs (J).

**Figure S9**

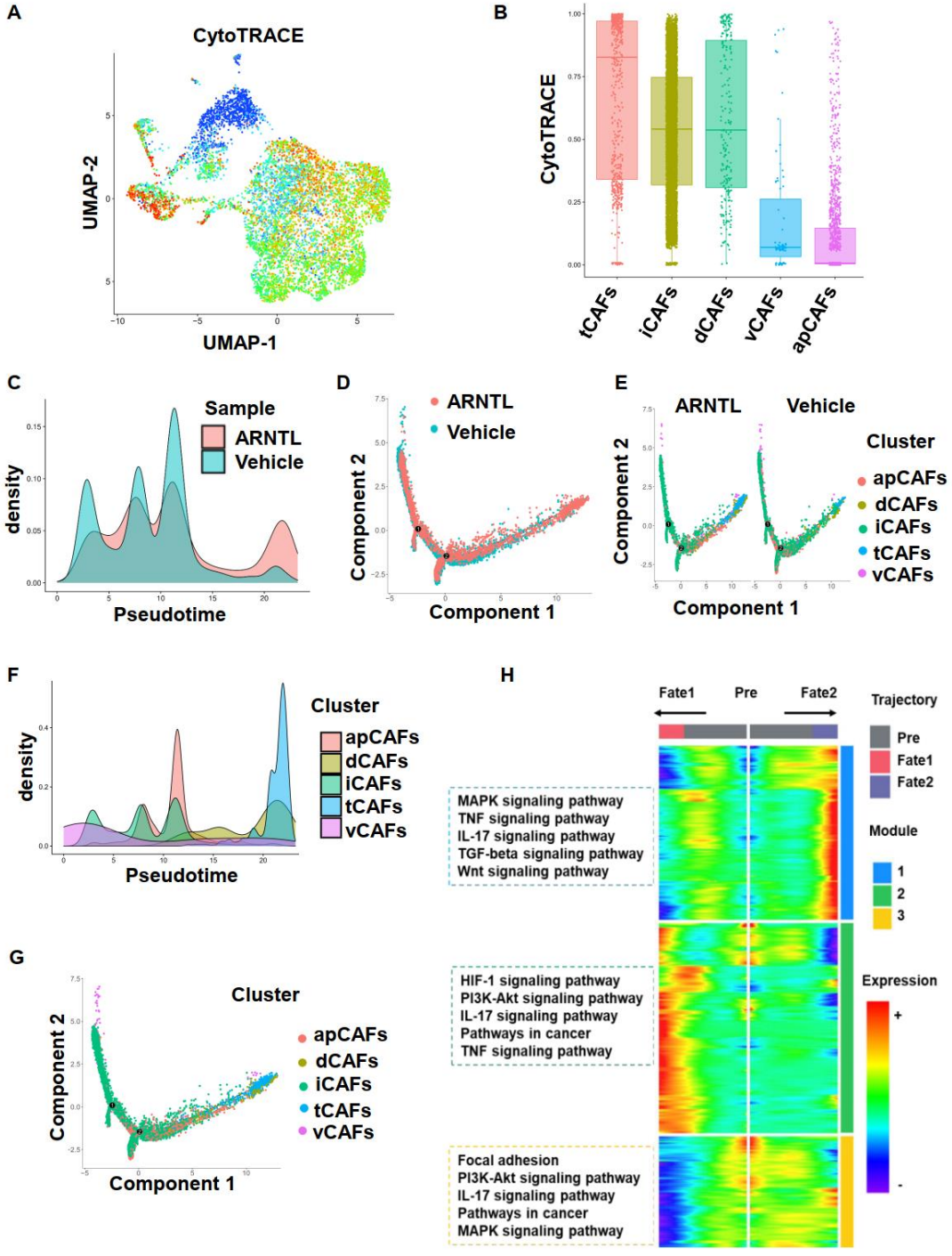

**Figure S9:** CytoTRACE and Pseudotime analysis in Fibroblast Classification of ovarian cancer. A, UMAP plot of CAFs cell stemness. B, Box plot of cell stemness in different CAFs. C, Probability density curve of Cell Distribution analyzed by in Vehicle and ARNTL. D, Scatter plot of Cell Distribution analyzed by in Vehicle and ARNTL. E, Density plot of pseudo distribution of various CAF cell types in Vehicle and ARNTL. F, Probability density curve of Cell Distribution analyzed in different CAFs; G, Scatter plot of Cell Distribution analyzed in different CAFs; H, Pathway analysis of key genes corresponding to the first node (mainly iCAFs and tCAFs).

# Figure S10

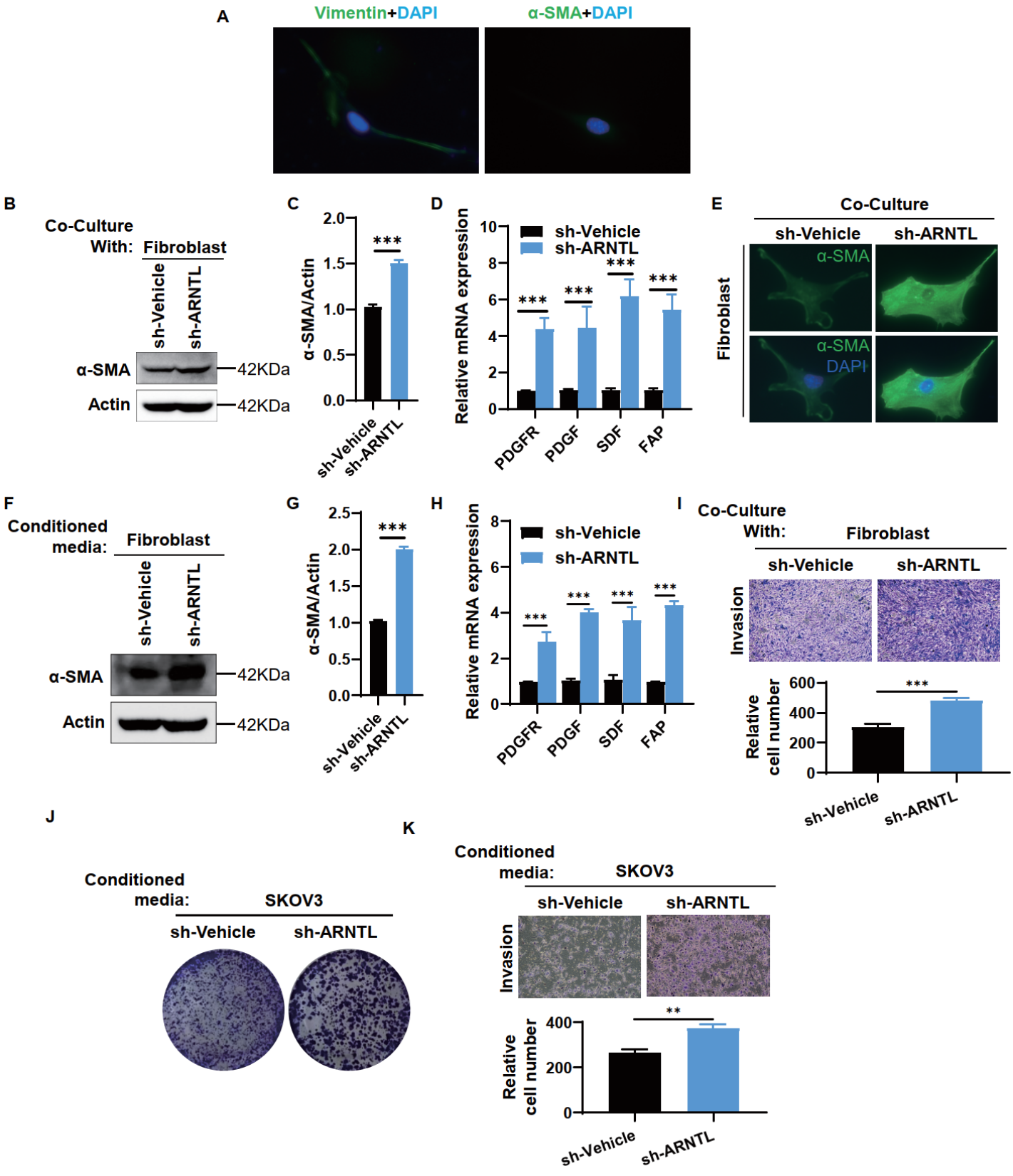
A
Vimentin+DAPI
α-SMA+DAPI
B
Co-Culture
With: Fibroblast
sh-Vehicle
sh-ARNTL
α-SMA
Actin
42KDa
42KDa
C
α-SMA/Actin
2.0
1.5
1.0
0.5
0.0
***
sh-Vehicle
sh-ARNTL
D
Relative mRNA expression
10
8
6
4
2
0
sh-Vehicle
sh-ARNTL
***
***
***
***
PDGFR
PDGF
SDF
FAP
E
Co-Culture
sh-Vehicle
sh-ARNTL
Fibroblast
α-SMA
α-SMA
DAPI
F
Conditioned
media:
Fibroblast
sh-Vehicle
sh-ARNTL
α-SMA
Actin
42KDa
42KDa
G
α-SMA/Actin
2.5
2.0
1.5
1.0
0.5
0.0
***
sh-Vehicle
sh-ARNTL
H
Relative mRNA expression
8
6
4
2
0
sh-Vehicle
sh-ARNTL
***
***
***
***
PDGFR
PDGF
SDF
FAP
I
Co-Culture
With:
Fibroblast
sh-Vehicle
sh-ARNTL
Invasion
Relative
cell number
600
400
200
0
***
sh-Vehicle
sh-ARNTL
J
Conditioned
media:
SKOV3
sh-Vehicle
sh-ARNTL
K
Conditioned
media:
SKOV3
sh-Vehicle
sh-ARNTL
Invasion
Relative
cell number
400
200
0
**
sh-Vehicle
sh-ARNTL

**Figure S10:** ARNTL inhibits the positive feedback regulation between cancer cells and CAFs. A, Representative immunofluorescence assays images for isolated fibroblasts, vimentin (left) and α-SMA (right) in fibroblasts. Cell nuclei were stained by DAPI (blue), scale bar: 20 μm. B-C, Western blot analysis for amounts of α-SMA in fibroblasts treated with indicated co-culture conditions for 48h. D, Real-time qPCR analysis for activation of fibroblasts treated in indicated co-culture systems for 48h. Values are mean±SEM. E, Representative images of immunofluorescence assay for α-SMA (green) or nucleus (DAPI) in fibroblast treated in indicated conditions for 48h, scale bar: 400μm. F-G, Western blot analysis for α-SMA activation in fibroblasts treated with indicated conditioned media for 48h. H, Real-time qPCR analysis for activation of fibroblasts treated with indicated conditioned media for 48h. Values are mean±SEM. I, Representative images of invasion cells (top), scale bar: 100μm. Relative numbers of invasion cells (down). Values are mean±SD. J, Representative images of colony formation assays of sh-ARNTL and sh-Vehicle for indirect conditioned media system. K, Representative images for Transwell invasion assays of SKOV3 cells after incubation with indicated conditioned media for 48h(top), scale bar: 100μm. Relative numbers of invasion cells (down). Values are mean ± SD.

# Figure S11

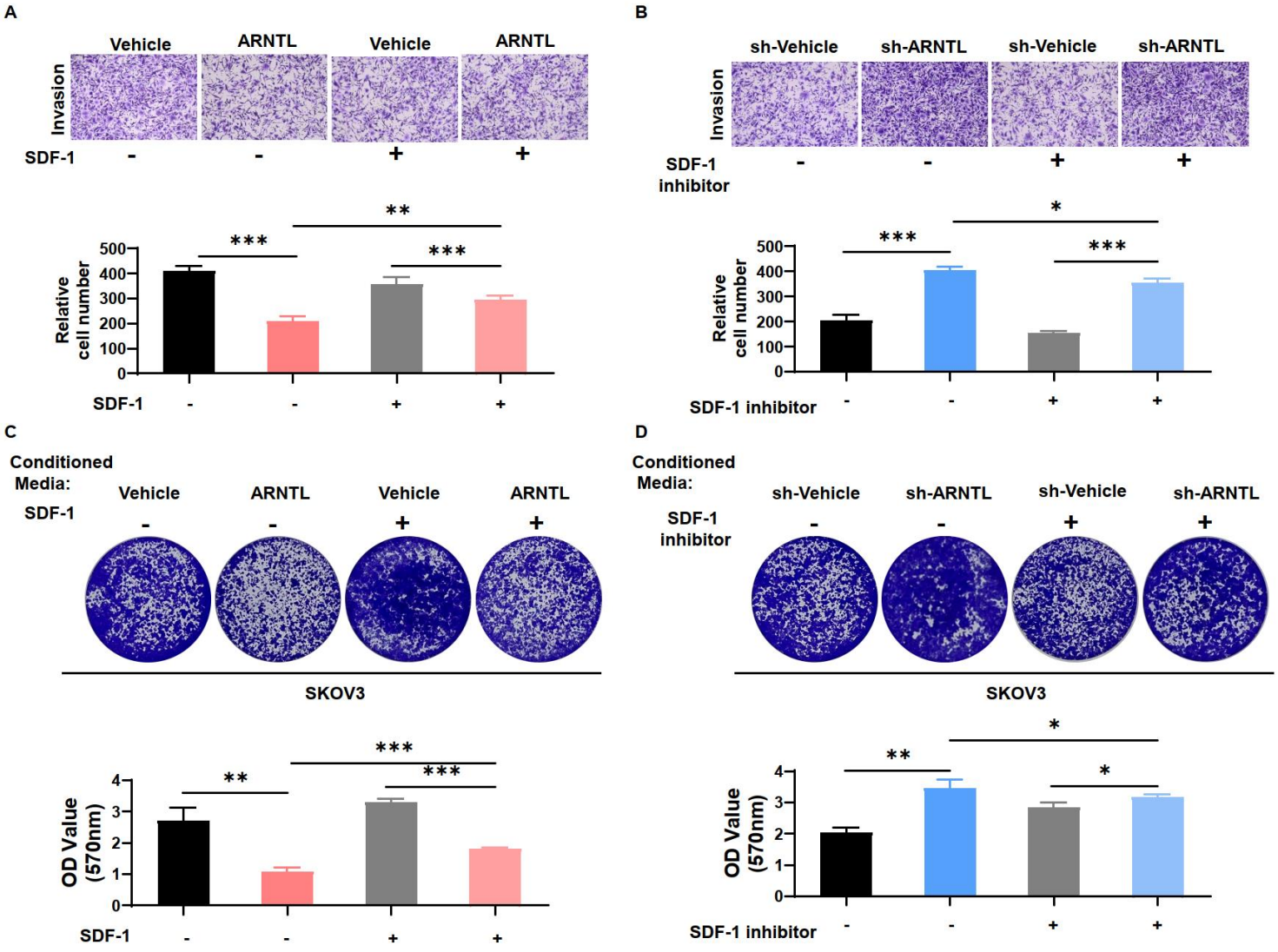
A
Vehicle
ARNTL
Vehicle
ARNTL
Invasion
SDF-1 - - + +
Relative cell number
SDF-1 - - + +
B
sh-Vehicle
sh-ARNTL
sh-Vehicle
sh-ARNTL
Invasion
SDF-1 inhibitor - - + +
Relative cell number
SDF-1 inhibitor - - + +
C
Conditioned Media:
SDF-1 - - + +
Vehicle
ARNTL
Vehicle
ARNTL
SKOV3
OD Value (570nm)
SDF-1 - - + +
D
Conditioned Media:
SDF-1 inhibitor - - + +
sh-Vehicle
sh-ARNTL
sh-Vehicle
sh-ARNTL
SKOV3
OD Value (570nm)
SDF-1 inhibitor - - + +

**Figure S11:** SDF-1-mediated ARNTL-CAFs axis regulation and functional recovery experiment. A, Representative image of Transwell invasion assay after 48 hours of incubation of SKOV3 cells with recombinant SDF-1 added to specified conditioned medium (top), scale bar: 100 μ m. The relative number of invading cells (decreased). The value is the mean ± standard deviation. B, Representative images of colony formation experiments with recombinant SDF-1 added to ARNTL and Vehicle indirect conditioned medium systems(top). The absorbance value of 570nm, the value is the mean ± standard deviation. C, Representative image of Transwell invasion assay after 48 hours of incubation of SKOV3 cells with SDF-1 inhibitor NOX-A12 added to specified conditioned medium (top), scale bar: 100 μ m. The relative number of invading cells (decreased). The value is the mean ± standard deviation. D, Representative images of colony formation assay with the addition of SDF-1 inhibitor NOX-A12 in sh-ARNTL and sh-Vehicle indirect conditioned media system(top). The absorbance value of 570nm, the value is the mean ± standard deviation.

**Supplementary Tables**

Table S1: The expression level of ARNTL across the examined ovarian cancer cell lines in the CCLE database.

Table S2: Gene Ontology (GO) analysis of co-DEGs identified between ARNTL vs Vehicle and sh-ARNTL vs sh-Vehicle conditions.

Table S3: KEGG analysis of co-DEGs identified between ARNTL vs Vehicle and sh-ARNTL vs sh-Vehicle conditions.

Table S4:The unique gene expression profile of cell types.

Table S5. Primers used for human qRT-PCR.

Table S6. Primers used for mouse qRT-PCR.